UNCLASSIFIED

AAEC/E52

AAEC/ E 52

AUSTRALIAN ATOMIC ENERGY COMMISSION

RESEARCH ESTABLISHMENT

LUCAS HEIGHTS

INITIAL RESULTS ON THE COMPATIBILITY OF AUSTENITIC STAINLESS-STEEL WITH CARBON-DIOXIDE

BY

A. DRAYCOTT

R. SMITH

First Issued Sydney, March 1960

Re-Issued Sydney, August 1960

UNCLASSIFIED

AUSTRALIAN ATOMIC ENERGY COMMISSION

INITIAL RESULTS ON THE COMPATIBILITY OF AUSTENITIC STAINLESS-STEEL WITH CARBON-DIOXIDE

by

A. DRAYCOTT

R. SMITH

Abstract

The possibility of selecting stainless-steel as either a canning or structural material in the projected Australian H.T.G.C. reactor has stimulated interest in the compatibility of this material with CO_2. The first series of experiments has been carried out on the oxidation behaviour of an 18-8-Ti stabilised steel in CO_2 in the temperature range 550-700^{o}C, under varying conditions of surface preparation, pressure, velocity and impurity content of the gas.

The rate of oxidation was followed by measuring the weight increase of specimens as a function of time of exposure in tests of up to 2500 hours duration. Supporting information on the nature of the oxidation process was obtained from metallographic and x-ray diffraction techniques.

It was found that work-hardened surfaces oxidised at a much lower rate than etched surfaces. In the case of work-hardened surfaces a protective film of Cr_2O_3 formed which persisted throughout the duration of the tests. On etched surfaces, rapid oxidation occurred to give a non-protective multi-layer scale.

In many specimens a thin layer of a second austenite formed below the oxide scale. In no case studied was there any evidence of carburisation.

Both pressure and velocity of the gas had considerable effects on the rate of attack of the steel.

This investigation has shown that in the ranges of pressure and velocity investigated, the 18-8-Ti austenitic stainless-steel can be used in CO_2 at temperatures up to 675^{o}C.

CONTENTS

(continued)

ILLUSTRATIONS (Continued)

1. INTRODUCTION

In the first report in this series (Draycott, 1959) the lack of information on the compatibility of stainless–steels with carbon–dioxide was clearly demonstrated. In addition to its possibilities for use as a structural material in the core of the High–Temperature Gas–Cooled (H.T.G.C.) reactor, and also in the hot gas ducting, 18–8–Ti austenitic stainless–steel may be used as the canning material.

Extensive studies have been made of the oxidation of stainless–steels in oxygen and air. However, all the work has been carried out at temperatures where the rate of oxidation obtained would be catastrophic for nuclear reactor applications. Work prior to 1953 has been reviewed by Kubaschewski and Hopkins (1953). More recently, the oxidation of stainless–steels has been studied by Edstrom (1957), Caplan and Cohen (1952, 1959) and Yearian et al (1956a, 1956b). Although these later studies go a long way towards explaining the mechanism of oxidation and the reasons for the oxidation–resistance, they are of little value in assessing the potentialities of austenitic stainless–steel in a carbon–dioxide cooled reactor at temperatures of the order of 550–700°C.

Very little work has been reported on the compatibility of stainless–steel with carbon–dioxide. McIntosh and Bagley (1955–1956) obtained no measurable weight–gain after five months in dry carbon–dioxide at 400° C. Huddle (1956) has claimed that all stainless–steels are resistant to oxidising gases below 600° C, but no experimental results were reported.

The work described in this paper is the first part of a detailed study of the behaviour of austenitic stainless–steels in carbon–dioxide in the temperature range 550–700°C. Although not complete, sufficient results have been obtained to assess the possible application of the metal as a canning and/or structural material in CO_2 cooled reactors in the temperature range mentioned.

2. EXPERIMENTAL METHODS

The steel used in all the experiments was a nominal 18–8–Ti stabilised austenitic stainless–steel in the annealed condition, with the following composition:

Carbon	0.12%
Silicon	0.08%
Phosphorus	0.027%
Chromium	18.2%
Nickel	10.5%
Titanium	0.38%
Molybdenum	0.72%
Manganese	1.22%

The carbon–dioxide was supplied by the Colonial Sugar Refining Co. Ltd., of Sydney. It was produced by the fermentation process and was of high commercial purity. The main impurity was air and concentrations of up to 200ppm oxygen and 800ppm nitrogen were encountered. The moisture concentration was usually below 50ppm. The only other impurities were the oxides of nitrogen and sulphur; these were present in only trace amounts, the concentration of sulphur dioxide never exceeding 3ppm while the concentration of nitrogen oxides was never greater than 0.1ppm.

Most of the work was carried out using CO_2 from 50 lb. cylinders. This resulted in appreciable variations in the oxygen content as the cylinders were emptied. In the later experiments the gas was supplied from a vessel of 6 tons capacity so that a reasonably constant level of impurities was maintained.

The variables which have been investigated to date are temperature (in the range 550–700°C), pressure (range 1–16 atmospheres) and surface preparation. Most of the experiments were carried out on the gas "as received", although a few have been performed using carbon–dioxide saturated with water vapour. In addition, some experiments on the effect of velocity of the gas have been made.

The different surface conditions tested were:-

(a) "as received" and degreased

(b) "as received" and etched

(c) "as received" and vapour-blasted

(d) ground to 400 grade on SiC papers

(e) ground and etched

(f) ground and vapour-blasted

Etching was done either in a nitric acid-hydrofluoric acid mixture ($HF:HNO_3:H_2O$ :: 15:1.5:83.5) at 55° C for 15 minutes or in a 50% hydrochloric acid solution at 70°C for 15 minutes. The vapour-blasting treatment used a high velocity jet of 400 grade Al_2O_3 in water, blown against the specimens.

Most of the tests were carried out in stainless-steel autoclaves of the type shown in Fig. 1. The pressure vessel was heated by a nichrome wire wound furnace, and temperatures were controlled to ± 5° C of the test temperature by means of a controller used in conjunction with a variable transformer. Specimens were hung from hooks welded to the thermocouple pockets. At least six replicate specimens were used in each test. The tests were all semi-static, with flow rates of 500 ml/minute at atmospheric pressure, to ensure that the composition of the gas in contact with the specimens remained constant.

The specimens used were usually 2cm square and 3mm thick giving a total surface area exposed to the gas of some 9-10 sq. cm. These specimens were removed from the autoclave at regular intervals and weighed. Tests of up to 2,500 hours were completed, although the normal duration was 1,000 hours. In a few experiments, new specimens were used each time so as to eliminate any thermal cycling effects; these proved to be negligible in our experiments.

The atmospheric pressure experiments were carried out in tubular resistance furnaces, temperatures being controlled in the same manner as for the autoclaves. Specimens were supported on silica boats and flow rates of up to 1 litre a minute were used.

The effects of the velocity were studied at atmospheric pressure in pumped loop, (Fig. 2). Heat was supplied by a nichrome wire-wound furnace and was removed by a water and air cooler used in series. Flow rates were measured by means of an orifice plate. The specimens used were rods approximately 3ins. long which fitted into the specially designed holder shown in Fig. 3. Velocities of up to 100 ft/sec. past the specimens were thus obtained.

The oxide scales on a number of specimens were examined using x-ray diffraction and metallographic techniques. In general, the x-ray diffraction analysis was done directly on the surface of the specimens using a Philips diffractometer.

3. EXPERIMENTAL RESULTS

3.1 Effect of Surface Preparation

The condition of the surface was found to have a marked effect on the rate of oxidation over the whole time of exposure used in these tests. This is illustrated in Figs. 4 and 5. Fig. 4 gives the results of tests carried out at 585-595°C and 150 p.s.i.g. on specimens in three different surface conditions - as received, etched, and vapour-blasted. Fig. 5 illustrates a similar effect obtained with specimens at 675-695° C and 150 p.s.i.g. In this case, the outer surface of the steel had been removed by grinding, and specimens were either mechanically polished (4A, 4B), ground and etched (4D), or ground and vapour-blasted (4C).

Etched surfaces showed weight-gains more than an order of magnitude greater than those from vapour-blasted surfaces. In the case of the etched specimens exposed at 680°C (4D), flaking of the scale occurred after about 500 hours exposure. Mechanically-polished specimens and those tested in the "as received" condition yielded weight-gains intermediate between those obtained from etched and vapour-blasted specimens.

The difference between the behaviour of the etched and vapour-blasted specimens was so striking that a detailed examination of the structure of the oxide scales was made on specimens 4A, B, C and D, Fig. 5. Two distinct types of oxide scale were observed, one type on the vapour-blasted specimen (4C) and the other type on the mechanically-polished (4A, 4B), and etched (4D) specimens; these were consistent in nature with the two types of scale A and B observed by Yearian et al (1956b) on chromium-nickel steels oxidised in air. On the vapour-blasted specimen, x-ray diffraction showed the presence of three oxide-phases, Cr_2O_3, Fe_2O_3, and a spinel of high lattice parameter. Other phases may have been present in small amounts, but as the average thickness of the film was 1-2 microns they would not be detected. This scale can be identified with the type A scale observed by Yearian et al, the formation of which was favoured by high chromium contents and low oxidation temperatures. They identified the high lattice-parameter spinel as $MnCr_2O_4$.

The structure of this scale is shown in Fig. 12 from which it may be seen that the distribution of the oxide phases is not uniform. Most of the surface was covered with a very thin oxide (less than 1 micron) which was assumed to be Cr_2O_3. However, there were localised regions of light-grey Fe_2O_3 on the surface, and also intrusions up to 10 microns deep of a dark-grey oxide; this phase must be $MnCr_2O_4$ or $FeCr_2O_4$. The heterogeneous distribution of Fe_2O_3 must be expected, since Fe_2O_3 and Cr_2O_3 are isomorphous.

The other type of scale, obtained on the mechanically polished, and etched specimens, is illustrated in Fig. 13. Three distinct layers of scale were observed. X-ray diffraction revealed the presence of only two structures, a rhombohedral structure with lattice parameter close to Fe_2O_3 (Di Carbo and Seybolt, 1959), and a cubic spinel structure of lattice parameter close to Fe_3O_4 (Yearian et al., 1954). The thin outer layer in Fig. 13 was identified as Fe_2O_3 on the basis of its colour (light-grey) and its anisotropic response to polarised light. The other two layers are both considered to be spinel structures, the reddish-grey intermediate layer being Fe_3O_4 and the dark-grey inner layer being a mixed Fe-Cr-Ni spinel. This interpretation identifies the scale as the type B scale observed on lower chromium steels particularly at higher oxidation temperatures by Yearian et al. The scale was up to 20 microns in thickness and where flaking had occurred it was confined mainly to the two outer layers.

Differences in the rate of oxidation and nature of oxide scales on the etched and vapour-blasted surfaces can be attributed mainly to the difference in work-hardening of the surface in the two cases. This was evident from the fact that specimens which had been etched after selectively work-hardening certain surfaces, showed very little scale-formation on the etched, work-hardened surface. Fig. 14 shows this effect on an etched specimen at the junction between the original surface and a sheared edge.

Specimens which did not have the original surface removed prior to vapour-blasting exhibited slightly different behaviour from those on which the original surface had been removed by grinding and polishing. The vapour-blasted "as received" specimens showed higher weight-gains and slightly thicker scales. Also, the scales were not as uniform and they did not exhibit such a well marked Cr_2O_3 phase. An example of this type of scale is shown in Fig. 15. One feature which was commonly observed was the presence of "warts" in the scale. These were localised regions where there had been a marked inward and outward growth of the scale. The structure of the scale within these warts appeared identical with the type B scale. These were not observed on the specimens which had been ground prior to vapour-blasting.

3.2 Effect of Temperature and Pressure.

In view of the much better oxidation-resistance of material with a vapour-blasted surface, the investigation of the effects of temperature and pressure was restricted to specimens in this initial condition.

The results of this investigation are shown in Figs. 6-9 in which the weight-gains of specimens are plotted as a function of time. A considerable scatter in the results was obtained, and for clarity, the curves have been drawn through points which represent the mean weight-gain of at least 16 specimens. From these curves it is clear that variations of temperature and pressure within the ranges investigated have significant effects.

An indication of the scatter is given on the curves; results fall within the ranges shown with a 66% reliability.

Based on the curves of Figs. 6-9, the rates followed the general equation:

$$\Delta W = kt^n$$

where ΔW is the weight gain in mgm/cm^2

k is the rate constant

and t is the time in hours.

The values of n and k were obtained for each set of conditions by plotting log ΔW against log t. These are shown in Table 1. From these results, n was found to vary over a fairly wide range from n = 0.6 to n = 0.2. At pressures of 225 p.s.i., the rate law was approximately parabolic but it approached a cubic law at lower pressures. (Alternatively, the results at lower pressures could have been fitted to a logarithmic law $\Delta W = k \log (at + b)$).

Normally the variation of oxidation rate with temperature is given by an expression of the Arrhenius type

$$k = A e^{\frac{-E}{RT}}$$

where A is the frequency factor

and E is the activation energy.

If the results of this investigation are fitted to a parabolic rate law and the logarithms of k plotted against 1/T, values of A and E are obtained; these are shown in Table 1.

No simple relationship could be found for the effect of pressure on the oxidation rates. At 575°C the oxidation rate is approximately proportional to $p^{1/2}$, at 615°C it is approximately proportional to p, and it was found to be proportional to a power of p greater than 1 at temperatures higher than 650° C.

The relationship of the weight-gains as a function of the variables pressure, temperature and time can be adequately expressed by

$$\Delta W = C e^{DP^{1.5}}$$

where P is measured in p.s.i.a.

D is a constant equal to

$$2.303 \times 10^{-4} \frac{mgm}{cm^2} \times \left(\frac{in^2}{lb}\right)^{1.5}$$

and C depends on the temperature and time.

The values of C for different values of temperature and time are shown in Fig. 10. Thus weight–gains may be calculated for specified temperatures and pressures in the ranges studied.

In order to calculate the amount of metal converted to oxide, the scale has been assumed to be of the formula M_3O_4. The atomic weight of M was taken as 54.3 and the density of the metal as 7.8 gm/cc. A period of 10,000 hours was chosen for this calculation so that an evaluation of the prospective long term use of this material for reactor purposes could be made. The results are given in Table 2, penetration depths being expressed in millimetres and thousandths of an inch.

Frost and Waldron (1959) have stated that at Calder Hall penetration depths of the Magnox can of between 0.00002 to 0.0001 in. per year are satisfactory. If these figures hold for stainless–steel, and if the effects of impurities and velocity are small then this material should be suitable for use either as a canning material or for structural purposes at temperatures up to 680–690°C with pressures of 10 atmospheres.

Using cans of 0.005 in. thickness an average loss of 0.00006 in. in 10,000 hours represents a decrease of only 1.2%. This should not significantly affect the mechanical strength of the material provided that there was no marked localised oxidation at any point on the surface.

Because of the thinness of the scales formed under all conditions of temperature and pressure, (average thickness $<$ 2 microns) it was difficult to establish the detailed differences in the structure of the scale brought about by changes in these two variables. Macroscopically, it was noted that the colour of the outer scale varied in a fairly well defined way with the weight–gains. For weight–gains below 0.05 mgm/cm^2 the scale was somewhat translucent and showed colours which varied through green, blue, red and orange. Between 0.05 and 0.15 mgm/cm^2 a uniform dark–grey surface was obtained and above 0.15 mgm/cm^2 a light bluish–grey scale formed, often only in patches. Microscopic examinations of sections through the scales showed only a dark irregular oxide ($<$ 1 micron) over most of the surface, Fig. 12. This type of scale was more uniform on all specimens exposed at lower temperatures and lower pressures; it was the only scale observed for specimens which had the original surface removed before vapour–blasting. This scale is considered to be mainly Cr_2O_3. However, on "as received" vapour–blasted specimens exposed at higher temperatures and pressures, the scales were less uniform and numerous warts (Fig. 15) were observed, together with regions where a slightly thicker uniform layer of a light grey scale existed (Fig. 16). Thus the increased weight–gains at higher temperatures and pressures were not clearly due to an overall increase in the thickness of the scale, but rather due to the presence of a greater number of warts.

3.3 The Effect of Velocity.

Although the velocity effect has not yet been completely investigated, sufficient results have been obtained to demonstrate the probable effect of this variable. Most of the experiments were carried out on vapour–blasted specimens, although two tests were completed on specimens with surfaces activated by pickling. Velocities of up to 105 ft/sec. were used and all tests were of 100 hours duration. The pressure in the loop during these tests was maintained slightly above atmospheric pressure.

The results are summarised in Table 3. The effect of velocity is very appreciable, particularly at the higher velocities of around 100 ft/sec. Sufficient results have not been obtained to derive any relationship between velocity of the gas and weight–gain of the specimens, but indications of the factor to be used in allowing for the velocity effect are shown in Fig. 11. In this figure the ratio of the weight–gain under dynamic conditions to the weight–gain at the same temperature and pressure in semi–static conditions is plotted against the velocity. There is an appreciable scatter of these plots but the straight line obtained by method of least squares is shown. Therefore, at a velocity of 100 ft/sec. (an approximate velocity expected to be encountered in the reactor) the weight–gain appears to be increased by a factor of 20 over the weight–gain encountered in semi–static conditions.

The mean penetration depth will, therefore, be increased by a factor of 20 and from Table 2 would result in a penetration of 0.00012 in. per 10,000 hours at a temperature of 695°C and a pressure of 225 p.s.i.g. This would be slightly higher than the allowances recommended by Frost and Waldron (1959). A safe working temperature under these conditions of velocity and pressure appears to be 675°C.

Since such a large effect of velocity is somewhat unexpected and difficult to explain, further extensive tests are in progress to verify this.

3.4 The Effect of Impurities in the Gas

A few experiments on the effect of moisture content of the carbon dioxide have been studied using gas at the saturated level (23,000 ppm) and in the commercially pure state ($<$ 50 ppm). The experiments were carried out at atmospheric pressure in tubular furnaces. Triplicate specimens were used in each test.

The results obtained are presented in Table 4, in which the ratio of the weight–gains of the specimen in "wet" gas to the weight–gains of the specimen in "dry" gas are shown at different temperatures and over varying periods of time. In all tests, greater weight–gains were experienced by the specimens in the wet gas, the ratio of $\frac{\Delta W_{wet}}{\Delta W_{dry}}$ usually being of the order of 1.3. This ratio varied little with time at any specific temperature. Although some tendency was noted for the ratio to be bigger at the lower temperatures, much more experimental data is required before the effect of moisture is fully understood. Nevertheless, complicated drying processes would not be required in the coolant circuit, providing the moisture did not have a detrimental effect on other materials present.

3.5 Other Metallographic Observations

Apart from the metallographic observations on the structures of the scales mentioned in 3.1 and 3.2 several other observations of interest were made.

As a result of the prolonged heat–treatment, there was a fine precipitate of sigma phase throughout the specimens. In the bulk of the specimens this precipitate was rather sparsely dispersed as fine particles at the grain boundaries. However, it was present in large amounts in regions which had been work–hardened prior to exposure in the temperature range 500–700°C. Thus precipitation was very marked near the drill holes, near sheared edges and close to the vapour–blasted surface, (Fig. 14.) The precipitate in these specimens was positively identified as sigma phase by x–ray diffraction and it was noted that there was no evidence of any carbide in the structure.

Associated with regions in which there was a dense sigma precipitate, a second fine–grained austenite phase was observed. This was also evident as a uniform layer 5 to 10 microns thick below the oxide scale on the vapour–blasted specimens except where there were warts, (Fig. 17.) It was identified as austenite by taking patterns on a Philips diffractometer of the oxidised surface. By comparing these patterns with the ones obtained after the oxidised surface had been polished away, it was established that this second austenite had a lattice parameter 0.14% less than that of the parent austenite.

This second austenite phase is considered to form mainly as a result of chromium removal from the matrix either by precipitation of sigma phase or by selective removal of chromium at the surface during oxidation (R. Smith, unpublished). The thickness of the layer near the surface is consistent with the available diffusion data for chromium in austenite at these temperatures.

4. DISCUSSION

The better oxidation–resistance of stainless–steels, compared with that of ordinary steels, is primarily a result of selective oxidation of the chromium to give a protective film of Cr_2O_3. This film is protective because the rates of diffusion of chromium and oxygen ions across the film are small, and also because it is coherent and mechanically stable. For similar reasons, oxidation protection is also claimed to be partly due to selective oxidation of Si to form SiO_2, (Caplan and Cohen, 1952) , and also to the formation of the spinel $FeCr_2O_4$ (Edstrom, 1957). However, the film produced by selective oxidation is metastable, and will tend to change to the more stable structure. Thus a Cr_2O_3 film will persist only as long as the rate of diffusion of chromium to the surface keeps pace with the rate at which the chromium is consumed by the oxidation reaction. Eventually there must be a breakdown of the Cr_2O_3 film leading to the formation of less protective but more stable phases. At high temperatures the breakdown will tend to occur after short exposure times (Edstrom, 1957). However, at lower temperatures, where diffusion rates are small, it may never be observed (Yearian et al 1956a).

Oxidation of stainless-steels at higher temperatures normally produces a scale consisting of a mixed Fe-Cr-Ni spinel, Fe_3O_4, and a Fe_2O_3 solid-solution (Edstrom, 1957; Yearian et al 1956b). This type of scale need not necessarily be preceded by the formation of a protective film of Cr_2O_3, as there is no reason why it should not be developed directly on the metal in a manner analogous to that observed on ordinary steels.

No marked differences in the oxidation-behaviour of stainless-steel would be expected when carbon-dioxide rather than air is the oxidising medium, provided that no difference in the nucleation characteristics is introduced. Oxidation in carbon-dioxide can be considered equivalent to oxidation in oxygen at very low pressures. For instance with carbon-dioxide which has a ratio of $CO_2/CO = 10^6$, the pressure of oxygen from the reaction

$$2CO + O_2 = 2CO_2 \; (\Delta G_0 = -135{,}100 + 41.50\,T \text{ cals/mole of oxygen})$$

is approximately 10^{-9} atmospheres at 700°C, and 10^{-16} atmospheres at 525°C (Richardson and Jeffes, 1948). (This is much lower than the pressure of oxygen impurity which, in our experiments, was of the order of 10^{-4} atmospheres). However, all the oxides that can be formed from stainless-steel have oxygen-dissociation pressures that are even less than this. Thus no difference in the equilibrium phases would be expected for oxidation in air and carbon-dioxide. Further, no marked differences should be obtained between the rates of oxidation of stainless-steel in these two media provided the same oxide phases form in each case. The rate of oxidation is primarily determined by the rates of diffusion of metal and oxygen ions through the oxide scales, and these should be the same if the oxide scales are the same. However, if carbon-dioxide was to favour the nucleation of, say, the protective rather than non-protective scale, then differences between the rates of oxidation in air and carbon-dioxide would be observed. At present such a comparison cannot be made but probably any differences observed would be less than those obtained in the present experiments by varying the surface condition.

The marked difference between the oxidation-rates of the work-hardened and etched surfaces in these experiments can be explained on the basis that work-hardening favours the nucleation of the protective Cr_2O_3 scale, whereas etching favours the nucleation of the less-protective oxides such as Fe_2O_3 and Fe_3O_4. It appears that once the protective film has been formed on the work-hardened surface it does not change much in constitution during tests of up to 1000 hours. However, further tests will have to be made to determine if there will be a breakdown of the film after longer times. A factor which must contribute to the stability of the protective film is that the diffusion co-efficient of chromium in the metal will have been increased by the plastic deformation of the surface layers during vapour-blasting.

The significant effects of pressure and particularly of velocity in these experiments is somewhat surprising, as these variables should not have marked effects on the rate of growth of a scale, if the rate-determining process is the diffusion of metal and oxygen ions through the scale. In the case of the velocity variable a marked effect would be expected if there was spalling of the scale, but this was never observed on vapour-blasted specimens. However, a possible explanation of these effects is provided by the results of the metallographic examination of the scales, namely, that the pressure and velocity of the gas are affecting the initial nucleation-process rather than the growth process. Apparently, with higher pressures and velocities, conditions are less favourable for the nucleation of the Cr_2O_3, and some nucleation of the non-protective scale occurs to produce "warts", (Fig. 15). Thus the increased weight-gains obtained at higher pressures and velocities are considered to be due to the greater number of "warts" of non-protective scale rather than to an overall increase in the thickness of one particular scale. This explanation is consistent with the fact that there was a wide scatter in the experimental results as this would be expected if pressure and velocity were affecting the nucleation stage rather than the growth stage. If correct, it means that there should be no effects from pressure and velocity if the surface were preconditioned at lower pressures to give first a uniform protective Cr_2O_3 film. This possibility is to be investigated.

Further experiments will also be carried out on other pre-conditioning treatments with the object of ensuring that a uniform protective film of Cr_2O_3 is always present before the steel is exposed to carbon-dioxide. By doing this, maximum oxidation-resistance should be obtained.

5. CONCLUSIONS

(1) If the surfaces of the material are work-hardened by vapour-blasting, 18-8-Ti austenitic stainless-steel can be used as a fuel-element canning material in commercially pure carbon-dioxide at temperatures up to 675°C at 15 atmospheres pressure and gas velocities of up to 100 f.p.s.

(2) Surface treatment of the steel prior to testing has a profound effect on its compatibility in carbon-dioxide. Etched specimens exhibit much greater weight-gains than specimens with work-hardened surfaces.

(3) Increases in both pressure and velocity of the gas lead to greater attack on the specimens.

(4) Increase in moisture content even up to 20,000 ppm has little effect on the rate of attack in carbon-dioxide.

(5) The effects of pressure, velocity and surface condition are considered to be due to the formation of different oxides in the initial nucleation stages, rather than to variations in the rate of growth of particular oxide-scales.

6. ACKNOWLEDGMENTS

The authors wish to express their gratitude to Mr. F.D.Nicholson for assistance in carrying out the exposure tests and the statistical analysis of weight-gain data, and to Mr. K.G.Watson for assistance with the metallographic and x-ray diffraction examinations.

7. REFERENCES

Caplan, D. and Cohen, M., 1952, J. Metals 4: 1057.

Caplan, D. and Cohen, M., 1959, Corrosion 14: 141.

Di Carbo, R.K. and Seybolt, A.U., 1959, J.Amer. Cer. Soc. 42: 430.

Draycott, A., 1959, A.A.E.C./K255.

Edstrom, J.O., 1957, J. Iron Steel Inst., 185: 450.

Frost, B.R.T. and Waldron, M.B., 1959, Nuclear Reactor Materials: p.68. Temple Press (London).

Huddle, R.A.U., 1956, 1st Nucl. Eng. and Sci. Congress, Cleveland, 1: 79.

Kubaschewski, O. and Hopkins, B.E., 1953, Oxidation of Metals and Alloys, Butterworths Scientific Publications (London).

McIntosh, A.B. and Bagley, K.Q., 1955-56, J. Inst. Metals, 84: 251.

Richardson, F.D. and Jeffes, J.H.E., 1948, J. Iron Steel Inst. 160: 261.

Yearian, H.J., Kortright, J.M. and Langenheim, R.H., 1954, J.Chem. Phys. 22: 1196.

Yearian, H.J., Randell, E.C. and Longo, T.A., 1956a, Corrosion 12: 515.

Yearian, H.J., Boren, H.E. and Warr, R.E., 1956b, Corrosion 12: 561.

TABLE 1

REACTION KINETIC DATA FOR THE REACTION OF

18–8–Ti AUSTENITIC STAINLESS–STEEL WITH CARBON–DIOXIDE

essure s.i.g.	Temp. °C.	Slope of Log–Log Plot n	Rate Constant for n = 0.5 k – mgm/cm²/hr ½	Frequency Factor A mgm/cm²/hr½	Activation Energy E Cals/mole metal
78	575	0.250	0.001521	19.34	15,640
	615	0.324	0.002818		
	655	0.417	0.00479		
	695	0.405	0.00586		
150	575	0.241	0.00228	47.4	16,740
	615	0.408	0.00389		
	655	0.304	0.00586		
	695	0.339	0.00765		
225	575	0.670	0.00282	176.4	18,780
	615	0.643	0.00501		
	655	0.569	0.00805		
	695	0.497	0.01120		

TABLE 2

CALCULATED PENETRATION DEPTHS IN 10,000 HRS.

Temp. °C	Pressure p.s.i.g.	Wt. Gain in 10,000 hrs. mgm/cm^2	Wt. Metal mgm/cm^2	Penetration Depth in 10,000 hrs.	
				mm x 10^4	0.001 in. x 10^3
575	78	0.1167	0.084	1.08	4.25
	150	0.1524	0.109	1.40	5.51
	225	0.2362	0.170	2.18	8.58
615	78	0.2671	0.192	2.46	9.69
	150	0.3492	0.251	3.22	12.68
	225	0.5411	0.389	4.99	19.65
655	78	0.5400	0.388	4.97	19.57
	150	0.7055	0.507	6.50	25.59
	225	1.093	0.785	10.06	39.60
695	78	0.760	0.546	7.00	27.56
	150	0.9929	0.713	9.15	36.02
	225	1.539	1.105	14.17	55.79

<u>TABLE 3</u>

RESULTS OF DYNAMIC COMPATIBILITY TESTS.

ALL EXPERIMENTS 100 HRS. DURATION.

Expt. No.	Temp. °C	Surface Finish	Velocity f.p.s.	Wt. Gain mgm/cm^2	Wt. Gain for Semi-Static Test (Fig. 15) mgm/cm^2
1	550	Pickled	59	0.82	–
		V.B.	14	0.03	0.009
		V.B.	9.5	0.01	0.009
2	550	V.B.	76	0.17	0.009
		V.B.	22	0.027	0.009
		V.B.	15	0.030	0.009
3	550	V.B.	54	0.185	0.009
		V.B.	13	0.033	0.009
		V.B.	8	0.028	0.009
4	550	V.B.	105	0.10	0.009
		V.B.	26	0.036	0.009
		V.B.	17	0.021	0.009
5	600	Pickled	61	1.07	–
		V.B.	15	0.09	0.022
		V.B.	10	0.04	0.022
6	600	V.B.	86	0.51	0.022
		V.B.	21	0.026	0.022
		V.B.	14	0.012	0.022
7	600	V.B.	57	0.10	0.022
		V.B.	14	0.038	0.022
		V.B.	9	0.038	0.022
8	600	V.B.	74	0.31	0.022
		V.B.	18	0.044	0.022
		V.B.	12	0.019	0.022
9	650	V.B.	83	0.52	0.037
		V.B.	20	0.049	0.037
		V.B.	13	0.034	0.037
10	650	V.B.	60	0.673	0.037
		V.B.	15	0.026	0.037
		V.B.	10	0.011	0.037

V.B. = Vapour–Blasted

TABLE 4

RATIOS OF WEIGHT-GAINS IN WET AND

DRY GAS AT DIFFERENT TEMPERATURES

Temp. °C	Values of $\frac{\Delta W_w}{\Delta W_d}$ after the following periods			
	250 Hrs.	500 Hrs.	750 Hrs.	1,000 Hrs.
575	1.45	1.42	1.49	–
625	1.38	1.39	1.45	1.46
675	1.32	1.29	1.29	–

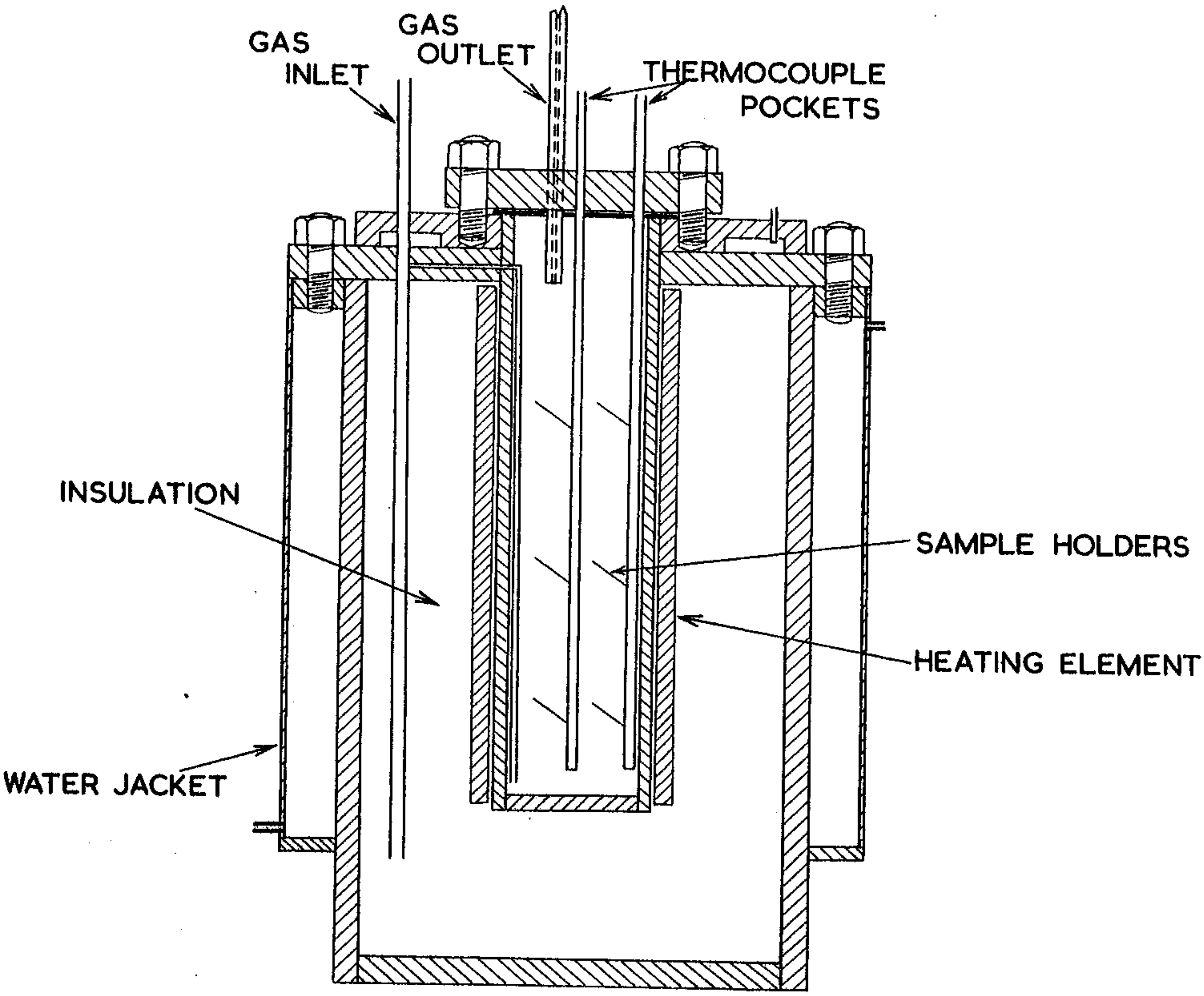

FIG. 1. AUTOCLAVE USED FOR PRESSURE EXPERIMENTS ON COMPATIBILITY OF AUSTENITIC STAINLESS STEEL WITH CARBON DIOXIDE.

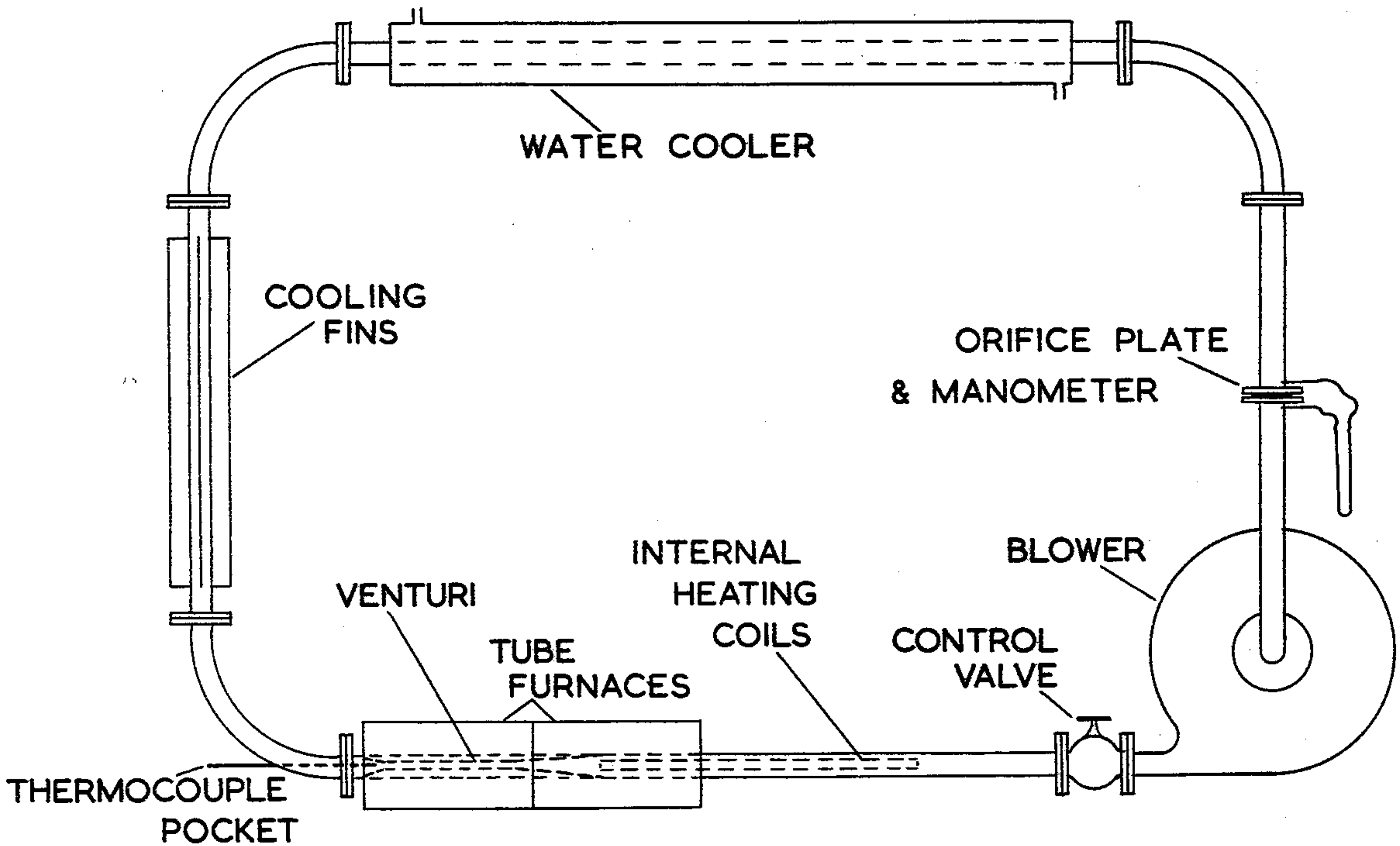

FIG. 2. LOOP USED TO STUDY THE VELOCITY VARIABLE.

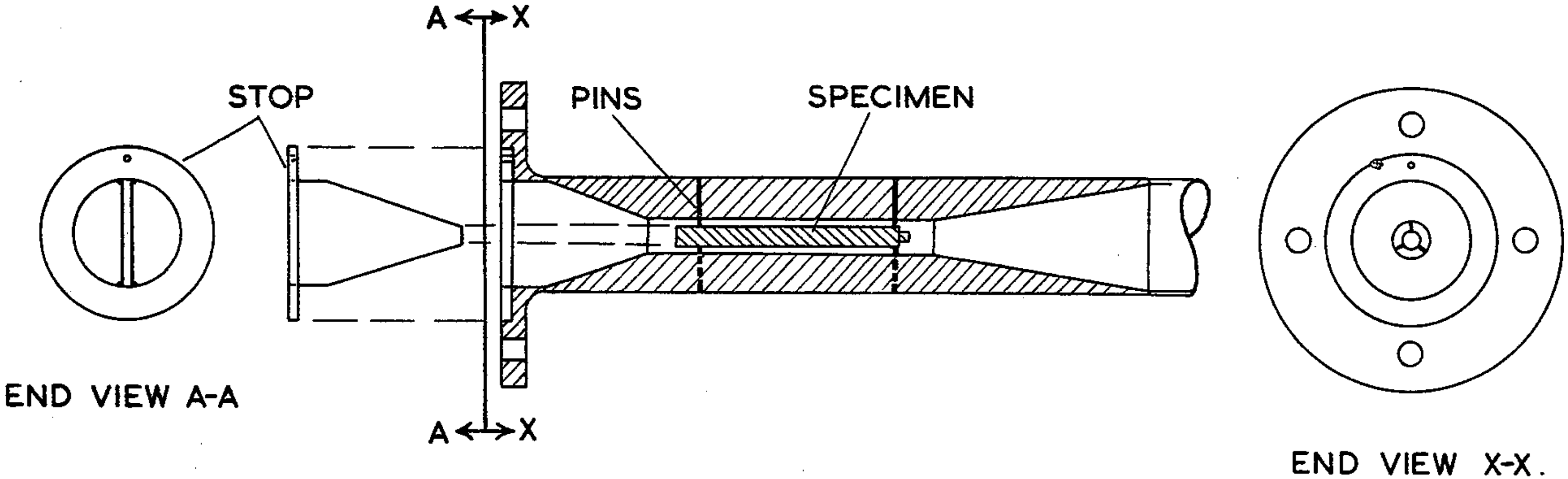

FIG. 3. SPECIMEN HOLDER IN DYNAMIC LOOP.

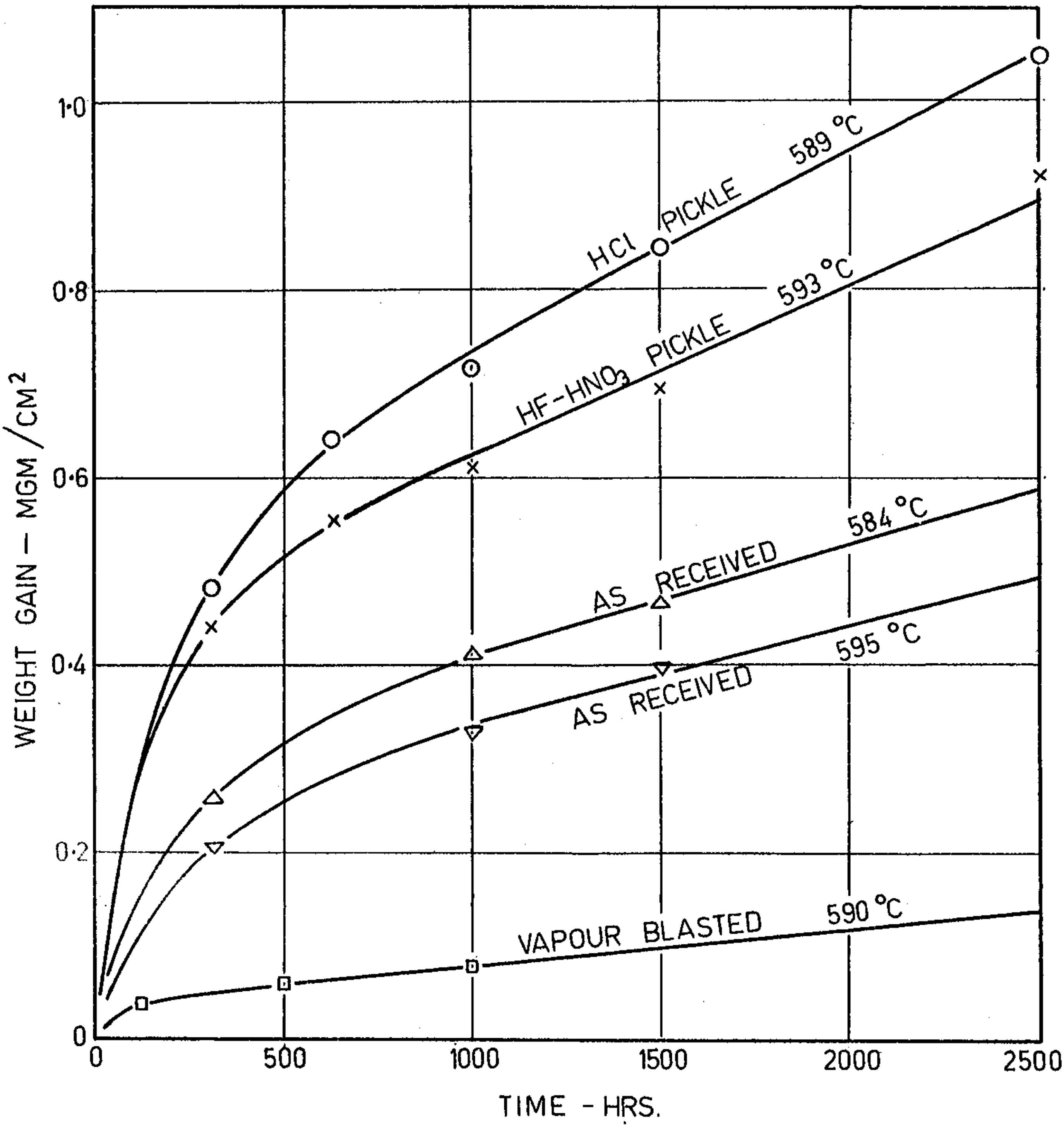

FIG. 4. THE EFFECT OF SURFACE TREATMENT ON THE WEIGHT GAINS OF AUSTENITIC STAINLESS STEEL SPECIMENS IN CO_2 AT 585-595 °C & 150 P.S

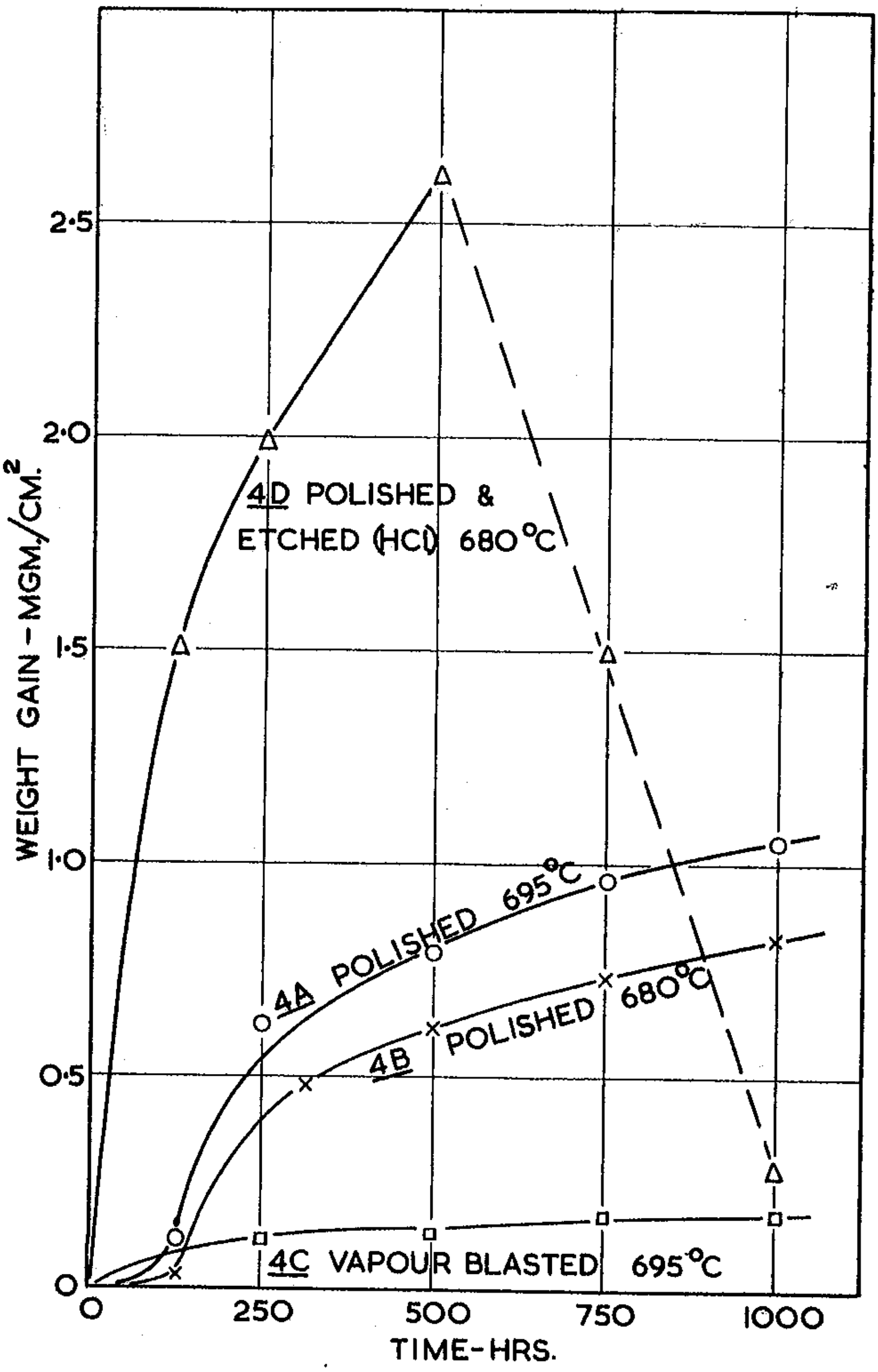

FIG. 5. THE EFFECT OF SURFACE TREATMENT ON WEIGHT GAINS OF AUSTENITIC STAINLESS STEEL AT 680-695°C & 150 P.S.I.G. IN CO_2.

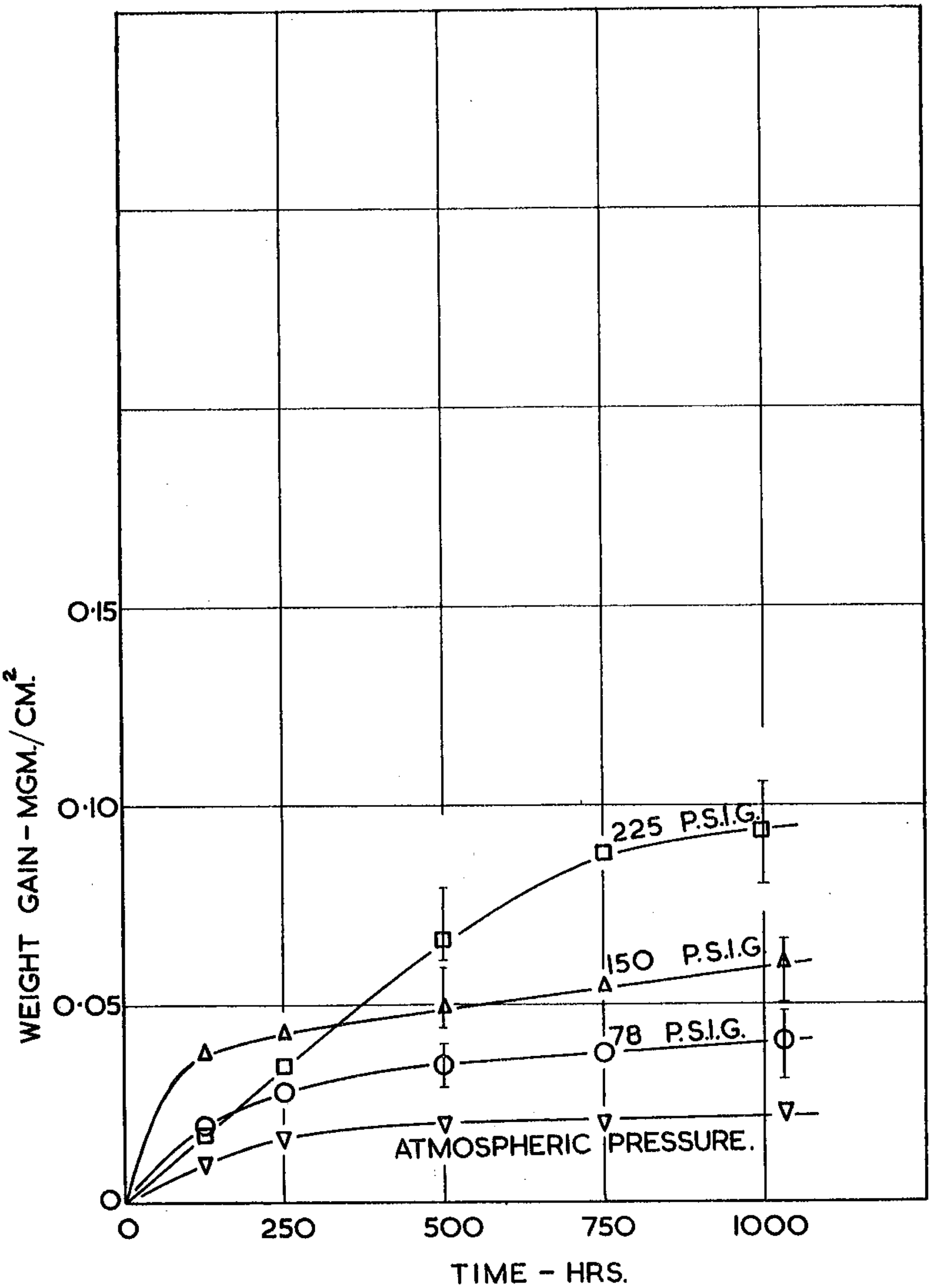

FIG. 6. WEIGHT GAIN DATA AT 575 °C.

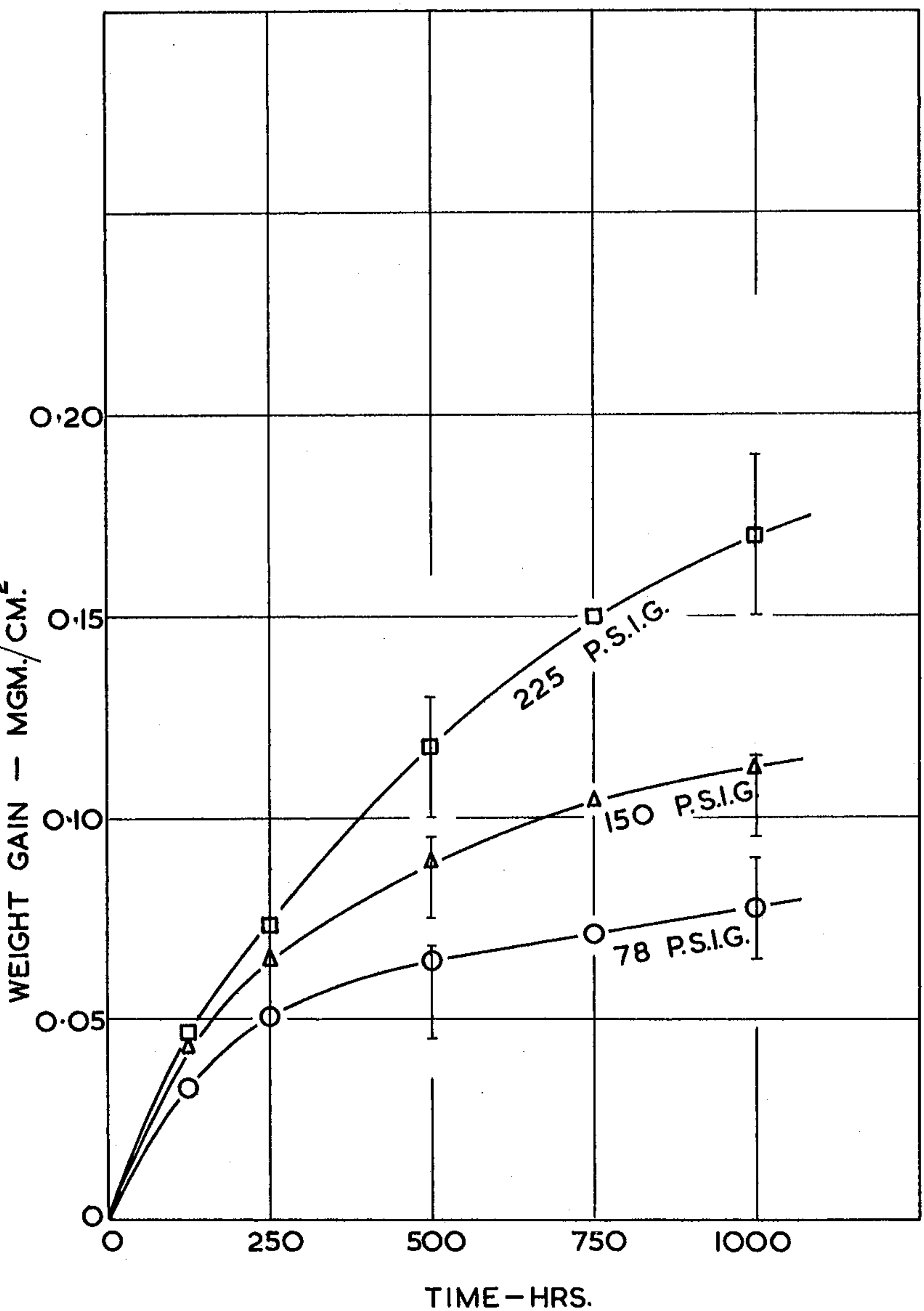

FIG. 7. WEIGHT GAIN DATA AT 615 °C.

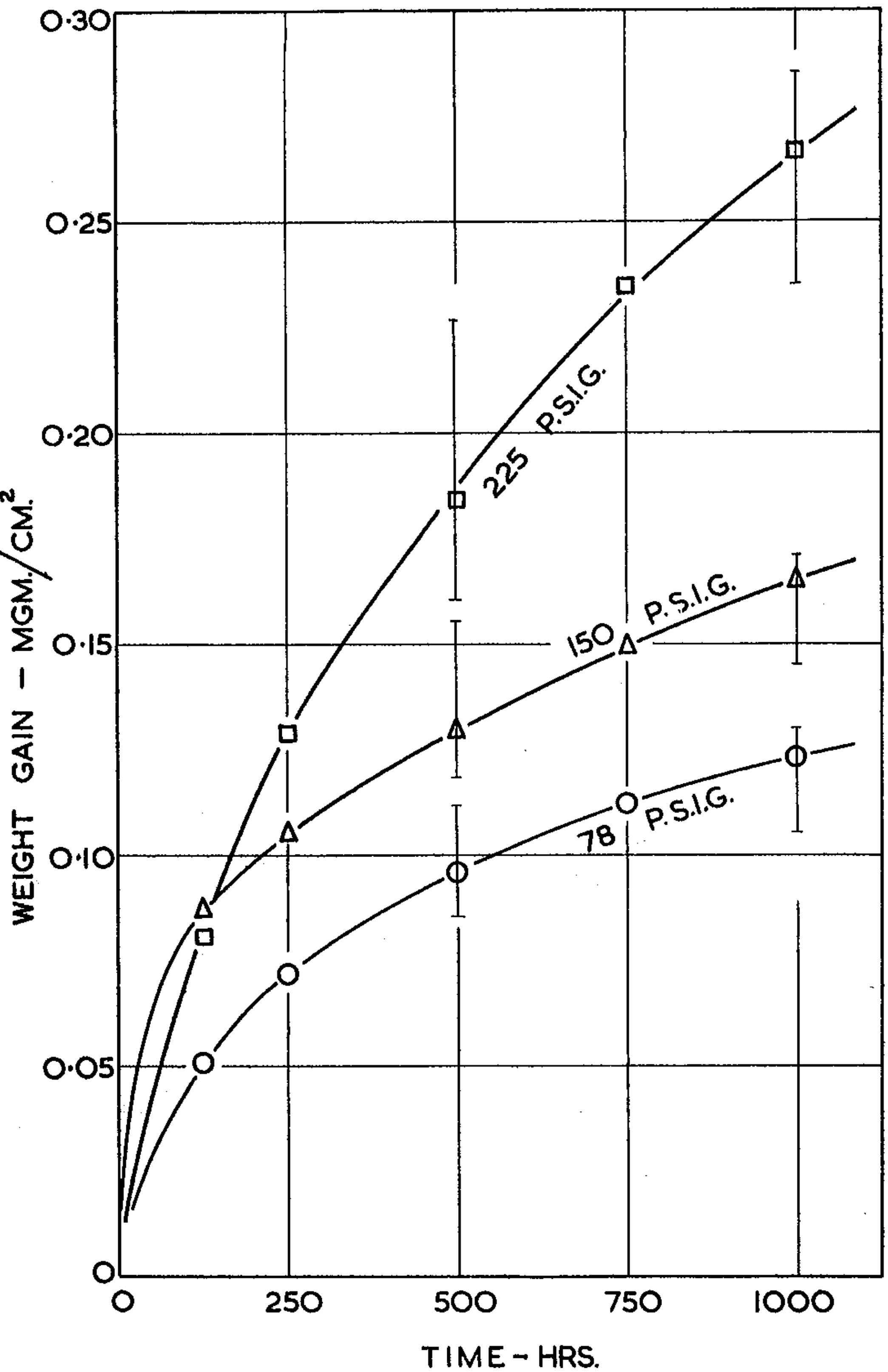

FIG. 8. WEIGHT GAIN DATA AT 655 °C

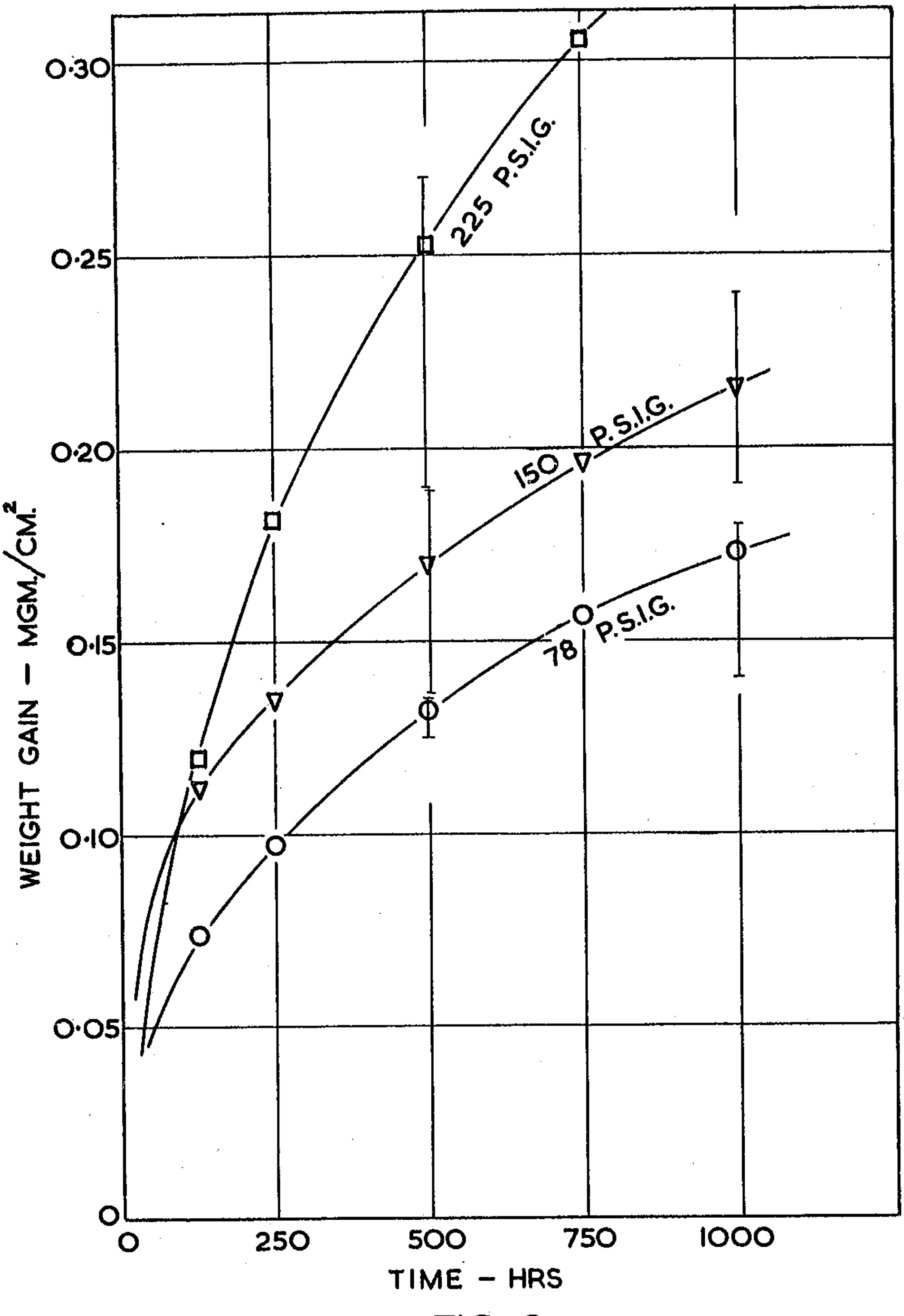

FIG. 9.

WEIGHT GAIN DATA AT 695°C

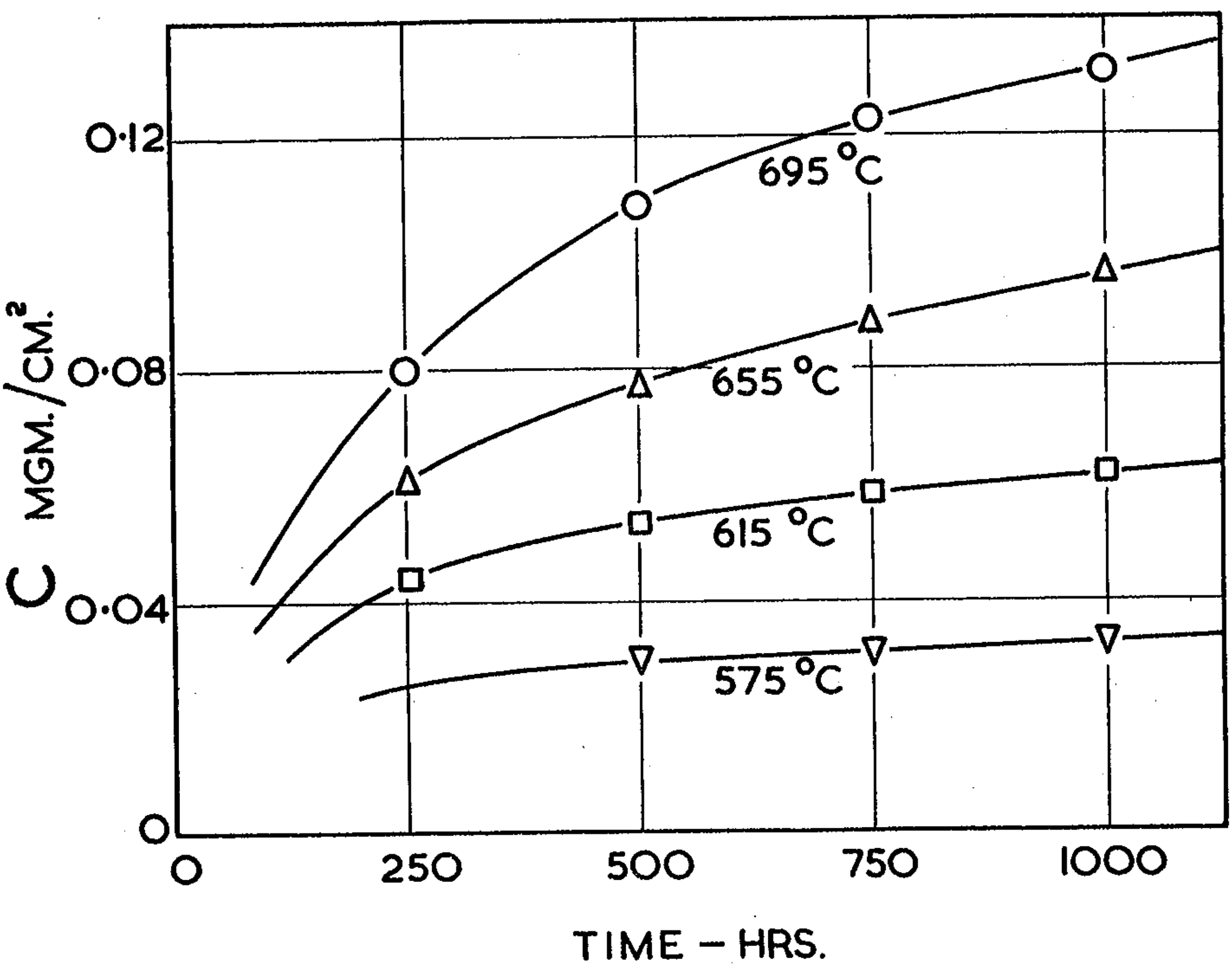

FIG. 10. VARIATION OF C IN

$\Delta W = C.e^{DP^{1\cdot5}}$ WITH TIME.

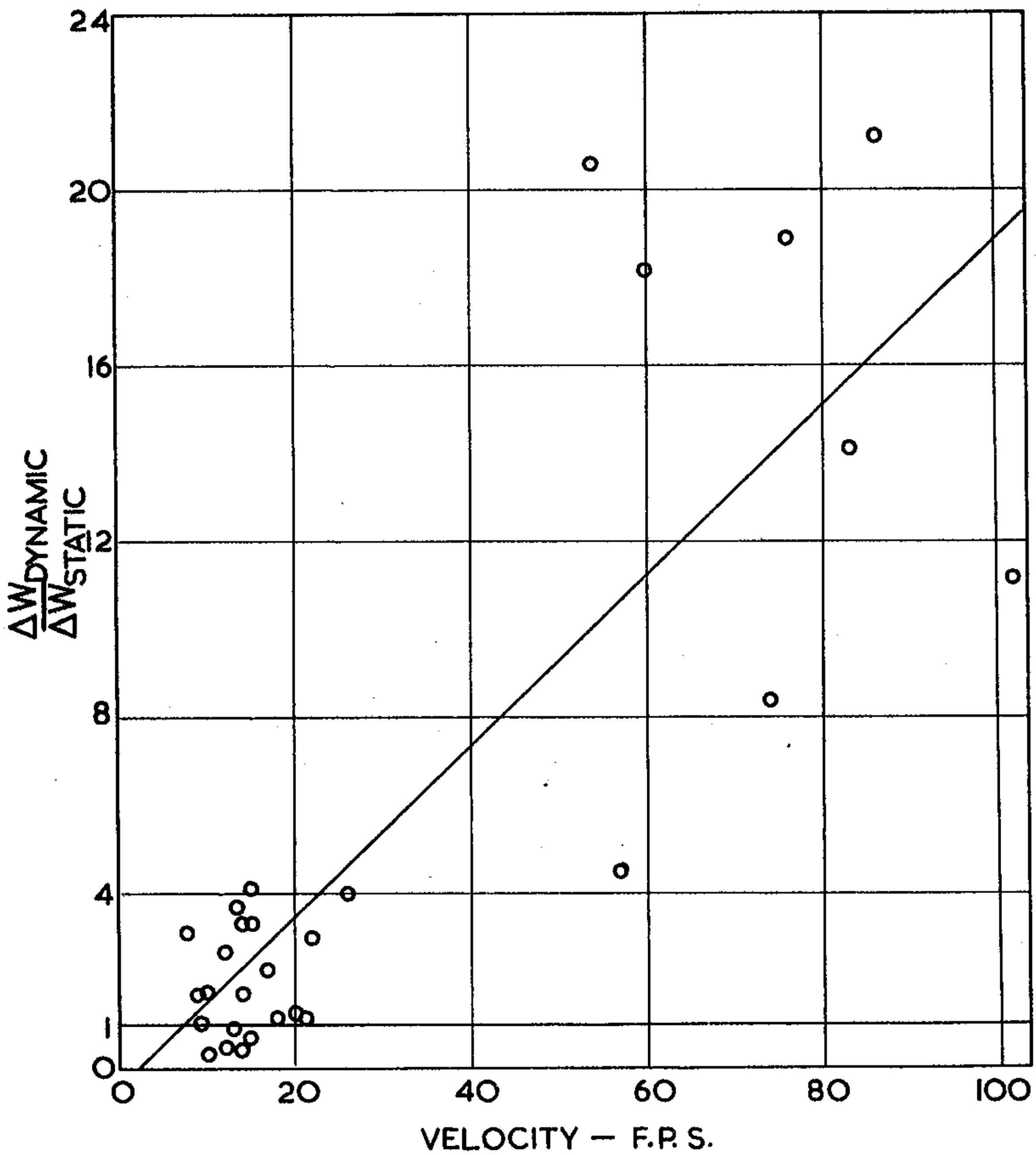

FIG. 11. WEIGHT GAIN DATA FOR DYNAMIC TESTS.

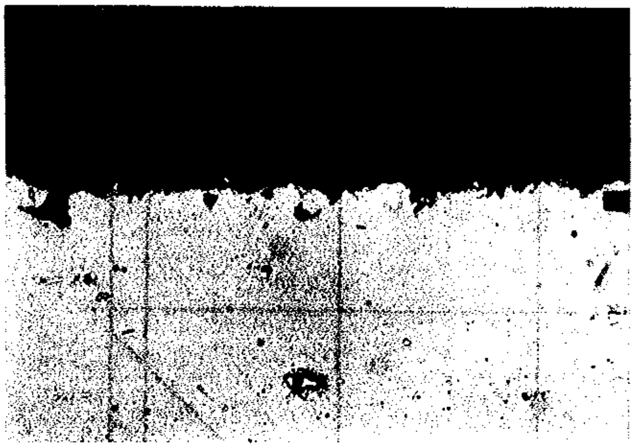

Fig. 12

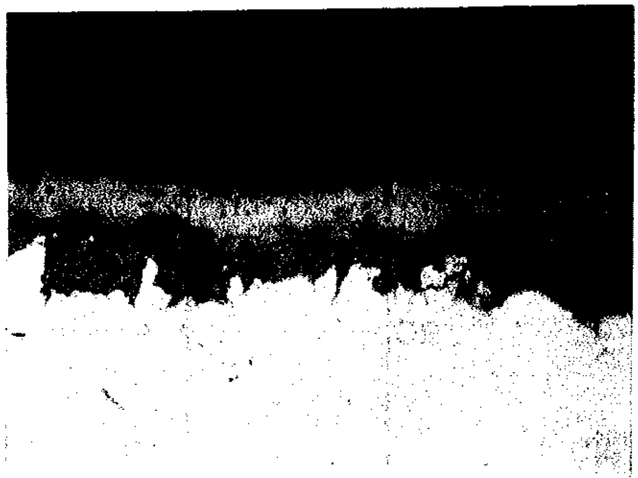

Fig. 13

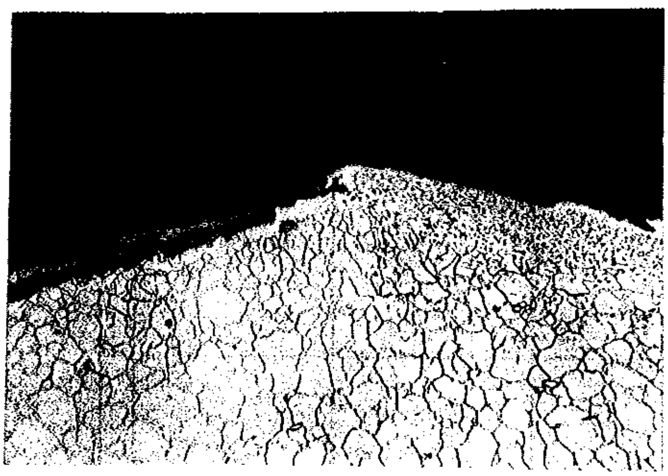

Fig. 14

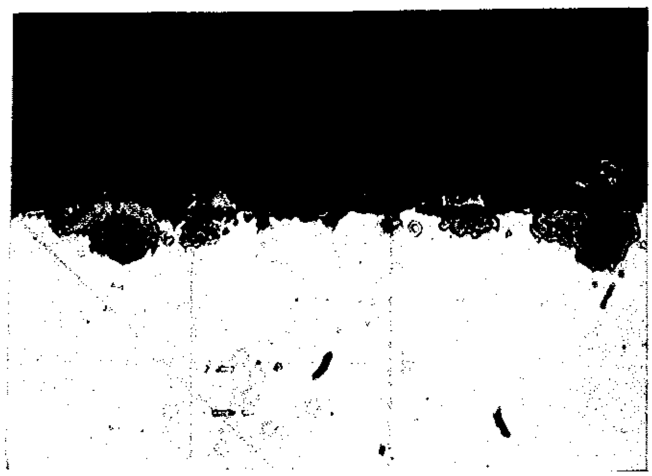

Fig. 15

FIGS. 12 – 15 : See explanation of figures in Contents.

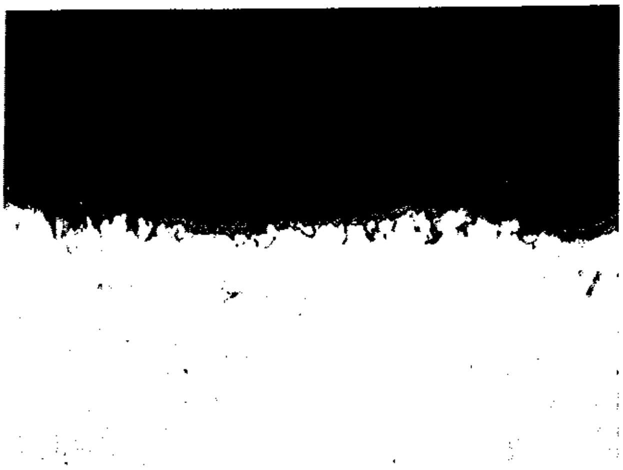

Fig. 16

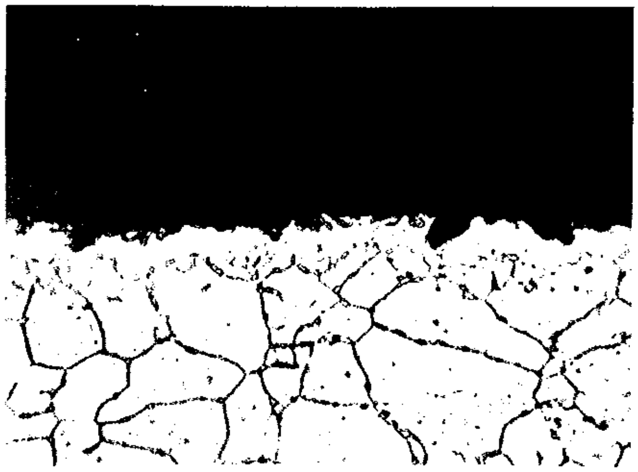

Fig. 17

FIGS. 16 – 17: See explanation of figures in Contents.